



HAL
open science

Effect of reactivity of different metakaolin mixtures on geopolymer extrudability

Wilfried Cyrille N'Cho, Paolo Scanferla, Anass El Khomsi, Guto Guido Da Silva, Guillaume Jamet, Ameni Gharzouni, Jenny Jouin, Sylvie Rossignol

► **To cite this version:**

Wilfried Cyrille N'Cho, Paolo Scanferla, Anass El Khomsi, Guto Guido Da Silva, Guillaume Jamet, et al.. Effect of reactivity of different metakaolin mixtures on geopolymer extrudability. *Journal of Building Engineering*, 2024, 86, pp.108990. 10.1016/j.jobbe.2024.108990 . hal-04792862

HAL Id: hal-04792862

<https://hal.science/hal-04792862v1>

Submitted on 20 Nov 2024

HAL is a multi-disciplinary open access archive for the deposit and dissemination of scientific research documents, whether they are published or not. The documents may come from teaching and research institutions in France or abroad, or from public or private research centers.

L'archive ouverte pluridisciplinaire **HAL**, est destinée au dépôt et à la diffusion de documents scientifiques de niveau recherche, publiés ou non, émanant des établissements d'enseignement et de recherche français ou étrangers, des laboratoires publics ou privés.



Effect of reactivity of different metakaolin mixtures on geopolymer extrudability

Wilfried Cyrille N'Cho, Paolo Scanferla, Anass El Khomsi, Guto Guido Da Silva, Guillaume Jamet, Ameni Gharzouni, Jenny Jouin, Sylvie Rossignol*

IR CER: Institute for Research on Ceramics (UMR CNRS 7315), European Center for Ceramics, 12 Rue Atlantis, 87068, Limoges, Cedex, France

ARTICLE INFO

Keywords:

Extrudability
Shaping
Metakaolin ternary
Mixture
Oligomers energy formation
Zeta potential

ABSTRACT

Additive manufacturing of geopolymers is an innovative technology for research and development. This work highlights the effect of different metakaolin mixtures reactivity on geopolymer extrudability. Extrudability tests were carried out on geopolymer pastes from different metakaolin ternary diagrams using two alkaline (potassium silicates K and sodium silicate KNa) solutions. Extrudable areas were delimited. To understand the differences, the reactivity of the different metakaolin mixtures was evaluated. The results showed that for the extrudable areas, the zeta potential values of the metakaolin mixtures ranged from -50 to -60 mV with K solution and were around -60 mV with the change of solution (KNa). Moreover, the extrudable area corresponds to an energy of oligomer formation (determined by thermal analysis) determined between 1.67 and 1.85 kJ mol⁻¹ with metakaolin ternary diagram M1-MI-M5 and 1.58 and 1.76 kJ mol⁻¹ for metakaolin ternary diagram M1-M2-M5. Whatever the alkaline solution used, the alkaline cation concentration of the extrudable domains is greater than or equal to 2.80 mol. L⁻¹. Mechanical strengths increase around 10 % from solution K to KNa. All these results are confirmed by using other aluminosilicate sources, such as argillite (clay calcined at 650 °C) and mixture of several clays (A650₃₀-M1₇₀ and A650₅₀-M1₅₀).

1. Introduction

Geopolymers are inorganic materials synthesized through the reaction of an aluminosilicate with an alkaline solution [1]. Among the aluminosilicate sources, metakaolin is the most reactive once in contact with the alkaline solution. The kinetics of the geopolymerisation reaction (dissolution of metakaolin by release of silicate and aluminate species, formation of oligomers by attack of Al species by alkaline solution silicates and polycondensation of oligomers) [2], can evolve according to the reactivity of the metakaolins. These behaviors control geopolymers properties in their fresh or consolidated state. Many works [3–5] were carried out on the impact of the reactivity of metakaolins in geopolymerisation reactions and highlighted that the most reactive metakaolins were characterized by good deshydroxylation, fast oligomer formation of the same nature, associated with low formation energies, leading to the formation of a homogeneous geopolymer network. In their fresh state, geopolymer pastes properties such as flowability or shaping linked to the reactivity of raw materials give them the possibility to be shaped by extrusion in additive manufacturing.

Additive manufacturing (3D printing) by extrusion is more popular in the construction industry [6]. The additive manufacture pastes involve a number of requirements linked mainly to the control of some properties in the fresh state, such as shape retention,

* Corresponding author.

E-mail address: sylvie.rossignol@unilim.fr (S. Rossignol).

optimisation of the open time (minimum time between two printed coats) and the stability of the mechanical properties of the extruded parts after setting [6,7]. These properties are governed by the reactivity of powder and the suspension.

Concerning geopolymers, several raw materials were used for 3D printing such as fly ash (FA), ground granulated blast furnace slag (GGBFS), silica fume (SF) [8–11], FA-GGBFS [12–15], FA-limestone [16], 100 % FA [17]. Furthermore, activators commonly used are combinations based on sodium or potassium silicate solutions [15,18,19]. Few authors have investigated the additive manufacturing of metakaolin-based geopolymer pastes [20–23]. Scanferla et al. [20] have evidenced the efficiency of pure geopolymer ink printing with the incorporation of ground geopolymer, which increased the yield strength and speeded up recovery after extrusion. Archez et al. [21,24] highlighted that 3D printing of geopolymers is possible without organics additives and with only mineral compounds by realizing a hollow cylinder ($\phi = 35$ cm, $e = 1,5$ cm, $H = 50$ cm) at $\frac{1}{2}$ scale. The stacking layers exhibited a good adhesion between them enabling the successful printing of hollow cylinders with flexural strengths of 15 MPa. Moreover, Zhong et al. [22] have shown that the presence of graphene oxide in geopolymer aqueous mixture dramatically changes its rheological properties, enabling the 3D printing of structures with compressive strengths over of 30 MPa and electrical conductivities of 10^2 S/m. According to Souza et al. [23] works, the 3D printing of metakaolin-based geopolymer pastes can be carried out, using a pre-heating system coupled to the printing nozzle, which makes it easy to pump very fluid mixtures. All these works evidenced that some parameters such as setting time, viscosity should be controlled. No data concerning extrudability of metakaolin mixtures has been investigated with this process. In previous works, the reactivity of different metakaolin mixtures and their impact on geopolymer properties has been evaluated [25,26]. The results revealed that the reactivity of metakaolins was linked to high amorphous and wettability values, as well as high zeta potential values (absolute value). These different characteristics of the metakaolins led to fast oligomer formation, and favored the formation of homogeneous geopolymer networks, whereas the less reactive metakaolins induced slow oligomer formation due to the presence of impurities, which led to the formation of different networks. However, the mechanical properties were not influenced by these characteristics but, working properties such additive manufacturing could depend on these different metakaolin characteristics.

The aim of this work was to investigate the feasibility of additive manufacturing of several formulations based on ternaries diagrams of metakaolins with different silicate alkaline solutions and without inorganic additive. In order to understand the extrudability of geopolymer pastes, zeta potential measurements were carried out on metakaolin mixtures, and the geopolymerisation reactions of the pastes were followed in situ by infrared spectroscopy (FTIR) measurements and thermal analysis. Finally, the mechanical strengths of the consolidated materials were investigated.

2. Experimental part

2.1. Raw materials and sample preparation

Raw materials used are grouped in Table 1. The aluminosilicate source used is made of mixtures of different metakaolins M1, M2 (supplied by Imerys), M5 (supplied by Argeco), a kaolin KI (Imerys) and argillite calcined at 650 °C (A650). Kaolin KI was calcined at 750 °C for 1h30 min in a rotary furnace to obtain metakaolin labelled MI [5]. As alkali activators, two commercial silicate solutions were used: K potassium silicate solution ($[K] = 5.0$ mol. L⁻¹) and KNa potassium and sodium silicate solution ($[K + Na] = 6.4$ mol L⁻¹) both provided by Woellner. The aluminosilicate source consisted on a mixture of M1 and M5 with MI or M2, based on the same % molar of aluminium (Fig. 1) as described in previous work [25]. The samples studied within the ternaries are denoted by the letters. For example, A₁ and A'₁ for K and KNa solutions used respectively (Fig. 1).

2.2. Methods of characterization

The determination of wettability consisted of the gradual application of drops of water, using a micropipette set on 10 μ l/drop, on 1 g of powder until it is completely wetted.

The extrudability behaviour was evaluated from qualitative tests. The experiments were carried-out extruding the geopolymer paste manually using a 30 cm³ plastic syringe (BD Plastik) with a tip diameter of 2.0 mm on Teflon supports. The investigation consisted on observations and pictures taken during or right after the extrusion. If the paste is easily extrudable, does not flow after the release of the pressure, namely dripping from the tip or having to dissipate the pressure that built to be extruded, and retains its shape once deposited, it can be considered extrudable. Otherwise, if the pressure is too high or too low, i. e. having a fluid or a highly elastic behaviour or being already consolidated, if after the extrusion the paste continues to drip from the nozzle or if once deposited on the substrate tends to lose its geometry, then it is not considered extrudable.

Raman spectroscopy was carried out on a T64000 Horiba-Jobin-Yvon spectrometer with a laser excitation of 514 nm operating at 30 mW. The backscattering mode was used with a long-distance objective (50 \times) and a triple diffraction grating (1800 lines/mm) to

Table 1
Nomenclature and composition of the different aluminosilicates sources.

Aluminosilicate source	Supplier	Weight composition (%)		Heating process
		SiO ₂	Al ₂ O ₃	
M5	ARGECO	59.9	35.3	Flash
M1	IMERYS	55.0	40.0	Rotary furnace
M2		55.0	39.0	Flash
MI		54.0	46.0	Rotary furnace
A650	ANDRA	57.1	15.7	Rotary furnace

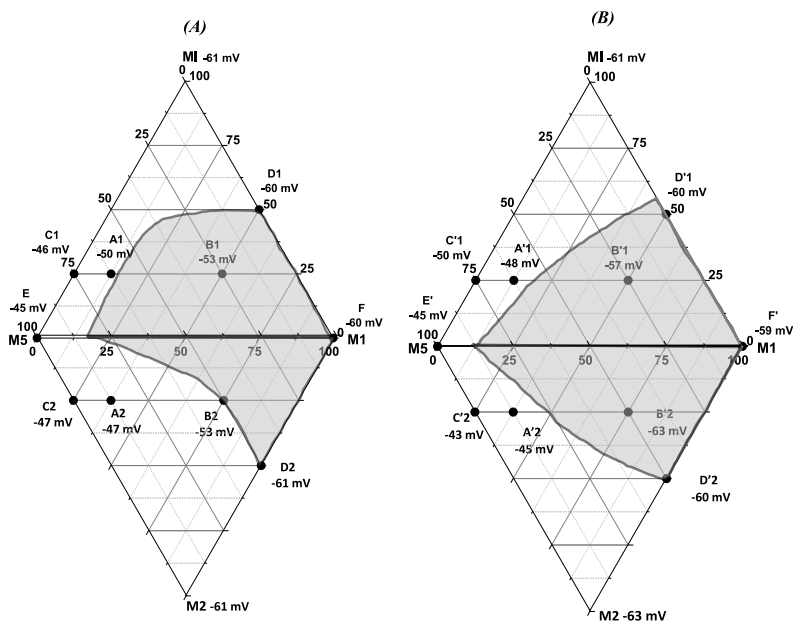

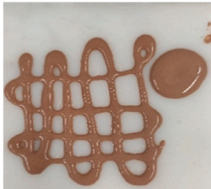








Fig. 1. (■) Extrudability and (□) non-extrudability existence domains and zeta potential values (± 5 mV) at pH = 11 of the ternaries (A) K/M1-M5-MI/M2, (B) KNa/M1-M5-MI/M2.

collect the scattered light. The spectral range was 200–1400 cm^{-1} with an accumulation exposure time (60) of 15 s. The spectra were corrected by baseline subtraction, modelled on a 5^o polynomial curve, and then decomposed with Wire software. The areas of the different contributions were calculated using Wire software.

Zeta potential is the electric potential developed at the shear plane of a particle dispersed in a liquid medium. The evolution of the zeta potential was monitored as a function of the pH values. First, a suspension of 0.25 g of the sample was dispersed in 25 mL of

Table 2
Examples of different geopolymer pastes (E_x) extrudable, (N. Ex) non-extrudable.

		Ternaries			
		MI-M1-M5		M1-M2-M5	
Solutions	K	 B1	 A1	 D2	 B2
	KNa	 B'1	 A'1	 D'2	 B'2
		E_x	N. E_x	E_x	E_x

distilled water by using a sonotrode for 90 s with 3 s intermittence. Then, the measurement of zeta potential was carried out with a Colloid Metrix Stabino II zetameter (Meerbusch, Germany). The pH values were modified using (1 M) solutions of K and KNa by adding a 15 μL volume of solution every 20 s.

Differential thermal analysis (DTA) and thermogravimetric analysis (TGA) were performed on an SDTQ600 apparatus from TA Instruments in an atmosphere of dry flowing air (100 mL/min) in platinum crucibles. The signals were measured with Pt/Pt-10 %Rh thermocouples. Thermal analysis was conducted during the formation of the consolidated materials using a thermal cycle previously established by Autef et al. [27]. The fresh reactive mixtures were maintained at 70 °C for 2 h. Analysis of the heat flux and its derivative allowed for the identification of all the samples properties and the delineation of four zones during the consolidation that could be attributed to the different stages of the geopolymerization process.

Infrared spectroscopy measurements were performed on a ThermoFisher Scientific Nicolet 380 in ATR (Attenuated Total Reflectance) mode. Acquisitions were made between 4000 and 500 cm^{-1} every 10 min for 12 h with 64 scans with a resolution of 4 cm^{-1} . OMNIC software (Nicolet Instrument) was used to acquire and process the data. The evolution of Si–O–Si (Q^2) bonds within the material is described by the superposition of the 72 spectra obtained. Thus, it is possible to plot the evolution of the Si–O–M band position ($M = \text{Si}$ or Al), translating the substitution of Si–O–Si bonds by Si–O–Al bonds in the geopolymer matrix [28].

Uniaxial compression tests were performed on cylindrical samples with an aspect ratio of 2 ($\varnothing = 15$ mm, $h = 30$ mm) after 7 days at room temperature. Instron 5969 with a load cell of 50 kN and a crosshead speed of 0.5 mm/min was used. The maximum compression strength σ_{max} was calculated by the means of seven samples for each composition and each temperature of treatment.

3. Results

3.1. Extrudability existence domains of several metakaolin mixtures

Extrusion tests were conducted with blends of metakaolins MI, M1, M2 and/or M5 and with two different silicate solutions K and KNa leading to four different geopolymer systems and the realization of four ternary diagrams based on aluminium moles percentages. Table 2 shows examples of extruded pastes with different aspects for the 4 ternaries. The criteria for which slurries are considered extrudable or not are based on observation of their behaviour during extrusion with the use of a plastic syringe (nozzle diameter of 2.0 mm) on a Teflon support. Fig. 1 shows the ternary diagrams resulting from the extrudability tests. Fig. 1 A-B shows the extrudability diagram of the geopolymer pastes produced with powders blends of MI, M1, M5 and M2 metakaolins. As shown, pastes produced with only one metakaolin were too fluid, and consequently non extrudable.

3.1.1. Ternary K/M1-MI-M5

The blend of M1 and M5 lead to enhanced extrudability until 80 % M5, while binary mixtures MI, M1 containing greater than 50% MI were not extrudable because the addition of a high proportion of MI induces shear thickening behaviour, making the paste difficult or impossible to extrude due to increasing resistance to the pressure applied.

Mixtures with the blend of MI and M5 are difficult to extrude, because they behave more like an elastic fluid resulting in a pressure build-up during extrusion and not allowing a homogeneous flow. The resulting pastes having a good extrudability for this first ternary diagram are B1 and as well as all points between F and D1. The formulations which define the limit of the zone of extrudability for the solution K and powder blends of MI, M1 and/or M5 are D1 and A1.

3.1.2. Ternary K/M1-M2-M5

Replacing MI with M2 metakaolin leads to different behaviours. First, M2 appears as an agglomerate powder, which makes the blending with either M1 and/or M5 difficult. In fact, it is easy to find, especially in blends made with M2 and M5, agglomerates of M2 coated with M5 powder. This has been observed to be a problem during the synthesis and the extrusion of some pastes. Second, at high content of M2, namely over 50 % mol, the paste produced has been observed to have a shear-thickening behaviour, which makes it difficult to mix and impossible to extrude, due to the increasing force in opposition to the extrusion pressure applied. Therefore, for a quantity of M2 below 50% mol, the obtained geopolymer pastes are observed to be more fluid than those produced with MI. Consequently, it is impossible to extrude pastes with mixtures of M2 and M5.

Mixtures of M2 and M1 (up to 50 %) have produced extrudable pastes. The formulations which are successfully extruded are limited by D2 and B2 points in KM1-M2-M5 ternary diagram. Their extrudability can be explained with the quick reaction rates of M1, which have already been observed [29].

3.1.3. Ternary KNa/M1-MI-M5

Unlike with K solution, pastes made with KNa solution resulted with a higher elastic behaviour and were generally more difficult to either mix or extrude (impossible; it is the case of E' and A'1 points). However, for proportions of less than 80% of M5 metakaolin in the mixtures, this phenomenon leads better extrudability with higher tendency to retain the shape after the extrusion and to not drip from the tip of the syringe without any force applied. M1 metakaolins and their blends emerged printable, likely due to the higher tendency of KNa solution to form elastic pastes. A high amount of MI tends to modify the pastes behaviour into shear-thickening, as seen for K solution. Blends made with MI and M5 yielded slurries that are non-extrudable, even when applying a limited quantity of MI metakaolin. On the other hand, blending MI with M1 seems to improve the extrudability, inducing the applicable amount of MI to the 55 %. Based on the KNa solution, extrudable pastes were made with MI, M1 and M5 metakaolins are M1, M5 and just above D2 point, which define the limits of extrudability for this ternary.

3.1.4. Ternary KNa/M1-M2-M5

The use of M2 with M1 and M5 on the KNa solution changes the behaviour of the pastes, as mentioned for K solution. In this case, pastes made only of M2 and mixtures M2-M5 can be not extruded from the syringe due to the strong elastic behaviour, which hinder the extrudability. However, decreasing its amount means decreasing the elastic behaviour favouring the fluidity making the pastes extrudable, with a well-defined extrudability zone including M1, M2, M5 and M1 at 50% (D/2). These pastes are the limit of the extrudability for the M1, and M2 metakaolins blend pastes based on KNa pastes.

To understand the extrudability of geopolymer pastes, the reactivity of the metakaolins corresponding to some formulations (extrudable or not) was evaluated by zeta potential measurements. Thus, the extrudable samples in ternaries with the K solution corresponds to metakaolin zeta potential values between -50 and -60 mV, while for the extrudable sample with KNa solution, the values are of the order of -60 mV. It is clear that the extrudability of geopolymer pastes requires the presence of a certain amount of reactive metakaolin species in solution in relation with zeta potential.

In order to understand the extrusion capacity of the blends, the reactivity of the precursors was highlighted by Raman spectroscopy measurements, especially on alkali silicate solutions, and zeta potential measurements for the metakaolins and blends. The difference in the zones of extrudability between the two solutions can be linked to the solutions reactivity. The obtained Raman spectra for the two silicate solutions in the range 200 – 1400 cm^{-1} are reported in Fig. 2. The silicon species can be found at 832 , 924 and 1046 cm^{-1} attributed to Q^0 , Q^2 and Q^3 , respectively, located on the same shifts for both solutions. Q^4 species, generally located at 1130 cm^{-1} [30, 31], are not observed. The TO/LO modes at 780 cm^{-1} , the M-O bonds at 325 cm^{-1} and the contribution attributed to the $\nu_{\text{Si-O}}$ monomer situated at 645 cm^{-1} are noted to be weak [32,33]. The bands corresponding to the tetrahedral rings R_3 , R_4 and R_5 are found at 598 , 480 and 440 cm^{-1} , while the Si-O-Si chains $C_{5,6,7}$ at 545 cm^{-1} . Comparing the two curves, the predominance of Q^0 and Q^2 Si species on KNa solution is visible and their presence is greater than those in K solution. Therefore, it is useful to evaluate the reactivity of a solution by comparison between the concentrations of the rings divided by that of the chains, as the ratio: $\log((R_3 + R_4 + R_5)/C_{5,6,7})$. As already stated in literature [32], solutions with high $\log(\text{rings/chains})$ ratio are noted to be highly reactive. In this case, K solution displays a ratio value of 0.68 , while KNa solution of 0.72 . Although the molar ratio between Si and alkali in both solutions is 0.8 , the overall total concentration of alkali is different. In fact, while the concentration of alkali in K solution is $[K] = 5.0$ mol. L^{-1} , for the KNa solution it is $[K + Na] = 6.4$ mol. L^{-1} . This means that there are more free alkali ions that participate to the reaction with the free Al and Si in system. A precedent study [34] on the reaction behaviours of geopolymers highlighted that the use of a silicate solution with a greater alkali concentration leads to quicker reactions. Moreover, Na-based geopolymers are noted to have reaction rates effectively quicker than K-based. These findings are in accordance with the observations carried out during the extrudability test, where the KNa solution was effectively noted be more reactive compared to K solution. Thus, a reactive alkaline silicate solution improves extrudability.

3.2. Mechanical properties

The compressive strength curves for some samples are shown in Fig. 3 and correspond to solutions K and KNa respectively. Table 3 shows the compressive strength values. Whatever the sample, the curves obtained show a linear variation characteristic of the elastic regime, followed by a slight plastic deformation and brittle failure [35]. The features of the KM1-MI-M5 based samples (A1, E, F) are similar and higher than the samples based on KM1-M2-M5 (A2). This behaviour can be attributed to the reactivity of the used solution in relation with the metakaolin. In fact, the same values obtained (around 65 MPa) are due to alkaline solution used [26]. The differences between the samples based on M2 or MI can be explained by the different reactivity of metakaolins mixtures. In presence of M2 metakaolin, there is a competition between the more reactive and less reactive metakaolins (M1 or M5) involving the oligomers formation. In fact, the presence of the alkaline solution induces a fast release of Al species from M2, which, delaying the release the aluminous species issued from M1 or M5. Consequently, the formation of several networks are responsible of mechanical properties loss. The change of solution increases the value of compressive strength (70 , 80 and 90 MPa for F', A'1 and E' respectively) linked to the

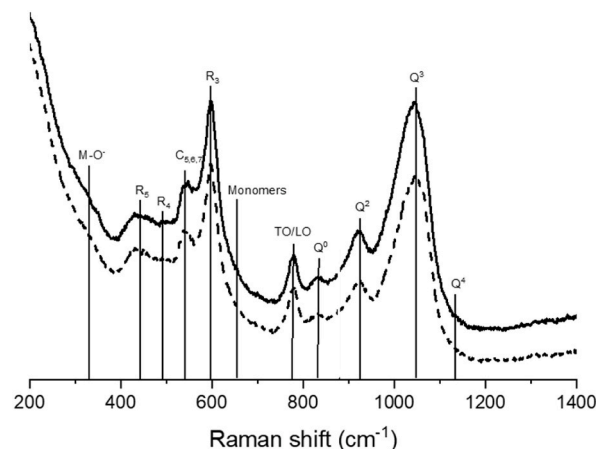


Fig. 2. Raman spectra (± 4 cm^{-1}) of the two solutions: (—) K and (---) KNa.

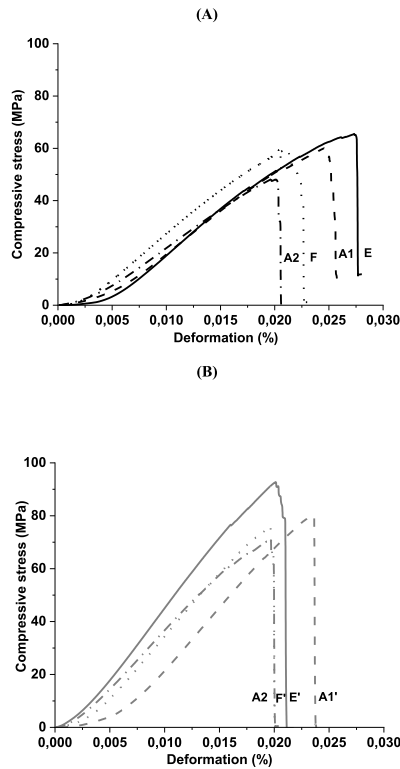


Fig. 3. Compressive stress value (± 5 MPa) as a function of deformation (± 0.001 %) for (a) (K) formulations and (b) (KNa) geopolymers formulations.

Table 3

Values of compressive strength for several samples of the four different ternaries diagrams, (*Italic*)extrudable points, (**Bold**) non-extrudable points.

Solutions	Ternaries	Samples	Compressive strength ± 3 /(MPa)
K	M1-MI-M5	<i>A1</i>	58
		<i>E</i>	65
	<i>F</i>	60	
	M1-M2-M5	<i>A2</i>	47
		<i>D2</i>	46
KNa	M1-MI-M5	<i>E'</i>	90
		<i>F'</i>	70
		<i>A'1</i>	80
	M1-M2-M5	<i>A'2</i>	70
		<i>D'2</i>	70

alkaline solution used. Moreover, the increase of the compressive strength of F' (from 60 to 70 MPa) could be explained by the fact that geopolymers based on metakaolin M1 and sodium silicate solution lead to higher performance than potassium silicate solutions [36]. The use of an alkaline reactive solution induces an increase in mechanical properties for metakaolin M1-based geopolymer [37]. Moreover, the differences observed, between E, F, and A1 are due to the impurities such as quartz. In previous works [29], it was demonstrated that using a sodium silicate solution with M1 increase the mechanical properties due to the high chemical binding affinity of Al species release with the Na cation. All these data underline the role of the reactivity of the alkaline silicate solution.

3.3. Some characteristics of selected formulations

In order to understand the differences in the ternaries, some formulations were selected. Data of the energy of oligomer formation and FTIR infrared spectroscopy are reported in Table 4 and supplementary file.

Fig. 4 shows the zeta potential data for metakaolins as a function of extrudability (1 = extrudable; 0.5 = non-extrudable) for the different M1-MI-M5 (Fig. 4A) and M1-M2-M5 (Fig. 4B) ternaries. Regardless of the mixture, extrudability limit values can be established for the different ternaries. These values are -50 and -60 mV for MI and M2-based ternaries respectively. These two limit values can be correlated with the reactivity of the solutions. KNa being more reactive, which results in a faster release of aluminous species compared to K solution. The non-extrudable formulations on the M1-MI-M5 ternary are those containing too much of M5 and MI

Table 4

Values of slope and oligomers energy of geopolymers samples; (*Italic*)extrudable points, (**Bold**) non-extrudable points.

Alkaline solutions	Ternaries	Samples	Slope ± 0.002 ($\text{cm}^{-1}/\text{min}$)	Oligomers formation ± 0.02 (KJ/mol)
K	M1-MI-M5	A1	0.019	1.79
		B1	<i>0.015</i>	1.71
		C1	0.025	1.86
		D1	<i>0.019</i>	1.76
		E	0.04	2.05
		F	<i>0.026</i>	1.8
	M1-M2-M5	A2	0.018	1.52
		B2	<i>0.02</i>	1.6
		C2	0.02	1.28
		D2	<i>0.03</i>	1.76
		E'	0.028	2.1
		F'	<i>0.013</i>	1.79
KNa	M1-MI-M5	A'1	0.027	1.99
		B'1	<i>0.016</i>	1.67
		C'1		
		D'1	<i>0.017</i>	1.84
		E'	0.028	2.1
		F'	<i>0.013</i>	1.79
	M1-M2-M5	A'2	0.02	1.15
		B'2	<i>0.016</i>	1.65
		C'2	0.025	1.16
		D'2	<i>0.023</i>	1.58

metakaolins due either to high water demand (due to MI metakaolin) or to the presence of impurities in the metakaolin (M5). The same observations are notable with M1-M2-M5 formulations with a higher quantity of M2. These zeta potential values highlight the quantities of reactive metakaolin species present in solution and therefore available to participate in polycondensation reactions. Consequently, the zeta potential values allow to determine the extrudability domain.

The oligomers formation energies were obtained by thermal analysis. In this work, the description of the thermal analysis curves refers to our previous work [26], which the curves and associated phenomena have been described. However, these curves can be found in the supplementary file All the values corresponding to the selected point are reported in Table 4. All the formulations of K/M1-MI-M5 ternary display values ranging from 1.71 to 1.86 kJ mol^{-1} except the for E point (2.05 kJ mol^{-1}). These values are related to the several networks due to the release of Al partially inhibited in relation with the impurities presents in the metakaolin mixtures [26]. The higher value of E sample is due to the presence of more impurities, which inhibit the Al release. The change of solution induces the same behaviour. As example of E' and B'1 sample with 2.1 and 1.67 kJ mol^{-1} respectively. The replacement of MI by M2 which is more reactive involves lower oligomer energies values due to the fast release of Al species (M2) only the D2 and B2 points remain extrudables due to the M1 presence (50 %). In presence of KNa solution, the extrudability zone becomes slightly larger than in the case of K due to the reactivity of KNa solution, however the D'2 point remains the extrudability limit with 1.58 kJ mol^{-1} . Thus, a range of geopolymer paste extrudability can be defined as a function of the oligomer energies and the different metakaolin ternaries. In fact, for the M1-MI-M5 ternary, the oligomers formation energy in the extrudable domain are ranging from 1.67 to 1.85 kJ mol^{-1} . For the M1-M2-M5, ternary, the oligomer formation energy of extrudable domain are ranging from 1.58 to 1.76 kJ mol^{-1} . The determination of oligomers energies formation could permit to predict also the extrudability of several mixtures.

In order to complete these analysis, in situ Infrared spectroscopy measurements were investigated, and the deduced slope were reported in Table 4. A higher slope value is characteristic of low formation of oligomers. Unlike, a low slope characterizes the fast formation of oligomers. In the K/M1-MI-M5 ternary, all extrudable points display a slope value are ranging from 0.01 to 0.026 $\text{cm}^{-1}/\text{min}$. The non-extrudable point E shows a slope of 0.04 $\text{cm}^{-1}/\text{min}$. The change of solution leads to the same behaviour. Indeed, the point E' is not extrudable with 0.028 $\text{cm}^{-1}/\text{min}$, whereas the extrudable point such B'1 displays a slope of 0.016 $\text{cm}^{-1}/\text{min}$. Using M2 metakaolin also lead to the same conclusion (0.02 and 0.016 $\text{cm}^{-1}/\text{min}$ for B2 and B'2 respectively). The determination of the slope value is also a method to evaluate the extrudability. All these different characteristics of metakaolin mixtures and geopolymer pastes show the existence of correlation between the extrudability of geopolymer pastes and raw materials reactivity.

4. Discussion

The knowledge of metakaolins characteristics such as zeta potential and the reactivity of silicate alkaline solution, is indispensable to understand the reactive mixture and especially the oligomers formation. In order to select a final mixture, all the previous data were plotted as a function of the alkali concentration [M] of the mixture in Fig. 5. The energies of oligomer formation (Fig. 5-A) the slopes of the geopolymers (Fig. 5-B) and the metakaolin mixtures zeta potential (Fig. 5-C), show two distinct areas as a function of the alkaline cation concentration. An area of extrudable points for alkali [M] ≥ 2.80 mol L^{-1} and another for [M] < 2.80 mol L^{-1} corresponding to the non-extrudable points area. These different observations could enable to establish an extrudability model linked mainly to the energies of oligomer formation, the slopes, the zeta potential values of the metakaolins and the alkaline cation concentration in the reaction mixtures. The validation of this model will require tests to be carried out with other aluminosilicate sources. Finally, extrudability tests were carried out with mixtures of calcined argillite (A650) [38] and M1 metakaolin (A650₃₀-M1₇₀ and A650₅₀-M1₅₀), and also the reactivity of the mixtures was evaluated. The results of extrusion tests are reported in Table 5. These results

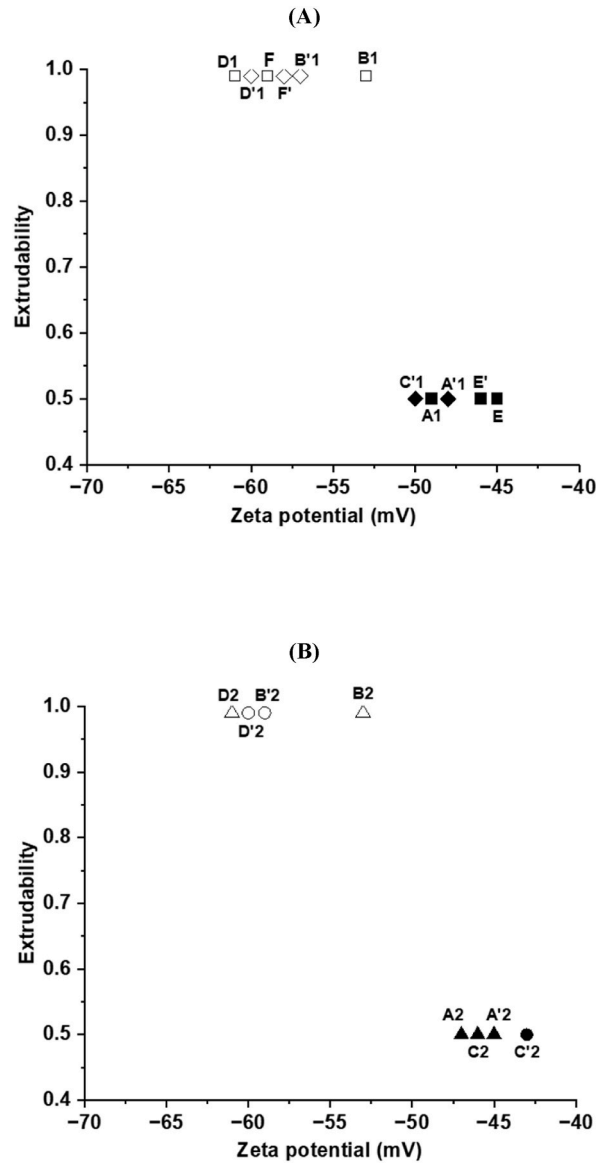


Fig. 4. Extrudability as a function of metakaolins zeta potential values (± 5 mV) for ternaries (A) K/KNaM1-M1-M5; (B) K/KNaM1-M2-M5; (∞ , \square , \circ , \triangle) extrudable; (\blacklozenge , \blacksquare , \bullet , \blacktriangle) non extrudable.

reveal that the use of K solution favors the extrudability of the two samples with alkali cation concentrations of 2.89 and 2.85 mol. L⁻¹ for A650₃₀-M1₇₀ (Ag₃₀) and A650₅₀-M1₅₀ (Ag₅₀) respectively. However, this is not the case with the change of solution (KNa). As expected, the samples KNa/A650₅₀-M1₅₀ and KNa/A650₃₀-M1₇₀ are neither extrudable nor castable due to the high reactivity of the KNa solution and of other components in the argillite [38] which induce fast setting of the geopolymer.

The metakaolins samples mixtures characteristics showed zeta potential values of around -50 mV for both mixtures regardless the alkaline solutions used. The argillite alone showed a zeta potential value -25 mV. The extrudable samples showed oligomer formation energies equal to 1.74 and 1.83 kJ mol⁻¹ for K/A650₃₀-M1₇₀ and K/A650₅₀-M1₅₀ respectively. In addition to that, the slope values obtained by FTIR spectroscopy are 0.017 and 0.022 cm⁻¹ for K/A650₃₀-M1₇₀ and K/A650₅₀-M1₅₀, respectively. These latest results confirm the results obtained in this work makes it possible to establish a model according to which the extrudability of geopolymer pastes is linked to metakaolin zeta potential values ranged between -50 and -60 mV, energies of oligomer formation ranging from 1.58 to 1.85 kJ mol⁻¹, slope values ranging from 0.010 to 0.026 cm⁻¹/min and an alkali [M] \geq 2.80 mol. L⁻¹. Finally, all these data enable us to establish an extrudability model for metakaolin-based geopolymer pastes as a function of the reactivity of the raw materials used.

5. Conclusion

This study was carried out to understand the additive manufacturing by extrusion of geopolymer pastes in relation with the

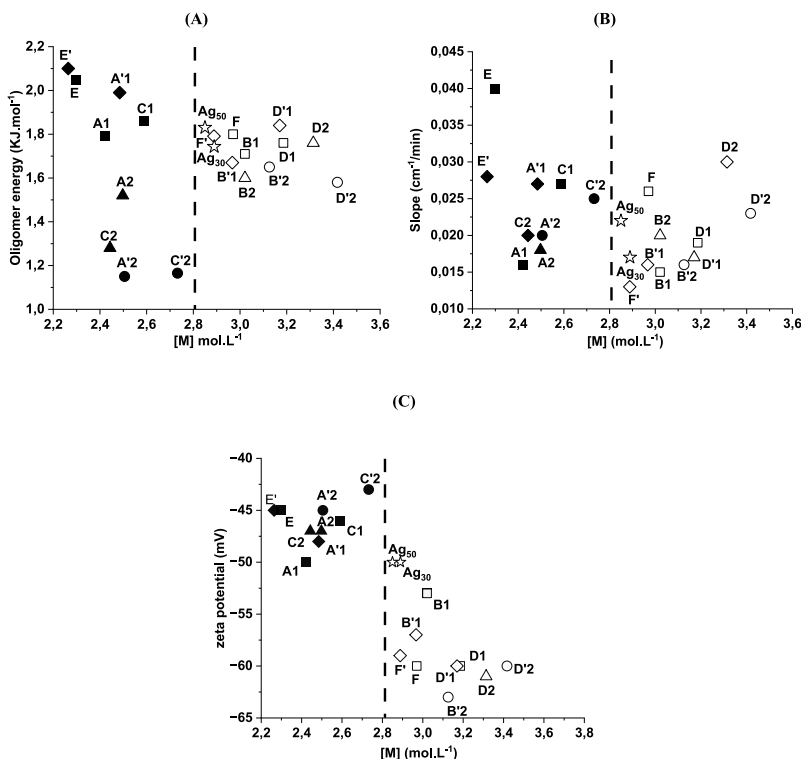






Fig. 5. Samples (a) slopes, (b) oligomer energies and (c) metakaolins mixtures zeta potential values as a function of alkaline cations concentrations ($\pm 0.05 \text{ mol. L}^{-1}$) for the all formulations; ($\circ, \square, \diamond, \triangle, \star$) extrudable; ($\blacklozenge, \blacksquare, \bullet, \blacktriangle$) non extrudable.

Table 5
Extrudability tests for samples A650₃₀-M1₇₀ and A650₅₀-M1₅₀ with K and KNa solutions.

Samples	A650 ₃₀ -M1 ₇₀	A650 ₅₀ -M1 ₅₀
K		
KNa		

reactivity of raw materials. Extrudability tests were carried out on different metakaolin blends obtained on the basis of two ternaries composed of MI, M1, M2, and M5 metakaolins using two alkali silicate solutions (K and KNa). Extrudability areas were delimited within the different ternaries K/KNa (M1-MI/M2-M5) as well as the energy of oligomer formation. The results highlight that.

- The use of K solution, results in zeta potential values are ranging from -50 to -60 mV and with KNa solution leads to zeta potential values around of -60 mV.
- The concentration of alkaline cations in the extrudable area is ≥ 2.80 mol. L⁻¹ whatever the alkaline solution used. The corresponding oligomer formation energies determined from thermal analysis are comprise between 1.67 to 1.85 and 1.58 to 1.76 kJ mol⁻¹ for the metakaolin mixture in M1-MI-M5 and M1-M2-M5, respectively. In the same way, the kinetic of oligomer formation ranged between 0.010 and 0.026 cm⁻¹/min for the extrudable zone.
- Mechanical strength was around 60 MPa with K solution and increase by around 10 % with KNa.

Finally, it has established that the extrudability domains are related to the different metakaolin mixture reactivity in relation with the alkali cation concentration. These new data were confirmed by other aluminosilicate sources.

CRedit authorship contribution statement

Wilfried Cyrille N'Cho: Formal analysis. **Paolo Scanferla:** Conceptualization. **Anass El Khomsi:** Data curation. **Guto Guido Da Silva:** Data curation. **Guillaume Jamet:** Methodology. **Ameni Gharzouni:** Validation. **Jenny Jouin:** Supervision. **Sylvie Rossignol:** Validation.

Declaration of competing interest

The authors declare that they have no known competing financial interests or personal relationships that could have appeared to influence the work reported in this paper.

Data availability

The data that has been used is confidential.

Appendix A. Supplementary data

Supplementary data to this article can be found online at <https://doi.org/10.1016/j.jobbe.2024.108990>.

References

- [1] J. Davidovits, *Geopolymer Chemistry and Applications*, Geopolymer Institute, 2008.
- [2] P. Duxson, A. Fernández-Jiménez, J.L. Provis, G.C. Lukey, A. Palomo, J.S.J. Van Deventer *Geopolymer Technology, The current state of the art*, J. Mater. Sci. Technol. 42 (2007) 2917–2933.
- [3] A. Gharzouni, L. Ouamara, I. Sobrados, S. Rossignol, Alkali-Activated materials from different aluminosilicate sources: effect of aluminum and calcium availability, J. Non-Cryst. Solids 484 (2018) 14–25.
- [4] V. Medri, S. Fabbri, J. Dedecek, Z. Sobalik, Z. Tvaruzkova, A. Vaccari, Role of the morphology and the dehydroxylation of metakaolins on geopolymerization, Appl. Clay Sci. 50 (2010) 538–545.
- [5] A. Autef, E. Joussein, A. Poulesquen, G. Gasgnier, S. Pronier, I. Sobrados, J. Sanz, S. Rossignol, Influence of metakaolin purities on potassium geopolymer formulation: the existence of several networks, J. Colloid Interface Sci. 408 (2013) 43–53.
- [6] S.C. Altıparmak, V.A. Yardley, Z. Shi, J. Lin, Extrusion-based additive manufacturing technologies: state of the art and future perspectives, J. Manuf. Process. 83 (2022) 607–636.
- [7] T.T. Le, S.A. Austin, S. Lim, R.A. Buswell, A.G.F. Gibb, T. Thorpe, Mix design and fresh properties for high-performance printing concrete, Mater. Struct. 45 (2012) 1221–1232.
- [8] M.K. Mohan, A. V Rahul, G. De Schutter, K. Van Tittelboom, Extrusion-based concrete 3D printing from a material perspective: a state-of-the-art review, Cem. Concr. Compos. 115 (2021) 103855.
- [9] R.A. Buswell, W.R. Leal de Silva, S.Z. Jones, J. Dirrenberger, 3D printing using concrete extrusion: a roadmap for research, Cement Concr. Res. 112 (2018) 37–49.
- [10] T. Wangler, N. Roussel, F.P. Bos, T.A.M. Salet, R.J. Flatt, Digital concrete: a review, Cement Concr. Res. 123 (2019) 105780.
- [11] J. Zhang, J. Wang, S. Dong, X. Yu, B. Han, A review of the current progress and application of 3D printed concrete, Compos Part A Appl. Sci. Manuf. 125 (2019) 105533.
- [12] G. Ma, Z. Li, L. Wang, G. Bai, Micro-cable reinforced geopolymer composite for extrusion-based 3D printing, Mater. Lett. 235 (2019) 144–147.
- [13] B. Panda, G.B. Singh, C. Unluer, M.J. Tan, Synthesis and characterization of one-part geopolymers for extrusion-based 3D concrete printing, J. Clean. Prod. 220 (2019) 610–619.
- [14] D.W. Zhang, D. min Wang, X.Q. Lin, T. Zhang, The study of the structure rebuilding and yield stress of 3D printing geopolymer pastes Constr, Build. Mater. 184 (2018) 575–580.
- [15] B. Panda, M.J. Tan, Rheological behavior of high-volume fly ash mixtures containing micro silica for digital construction application, Mater. Lett. 237 (2019) 348–351.
- [16] H. Alghamdi, S.A.O. Nair, N. Neithalath, Insights into material design, extrusion rheology, and properties of 3D-printable alkali-activated fly ash-based binders, Mater. Des. 167 (2019) 107634.
- [17] B. Panda, C. Unluer, M.J. Tan, Extrusion and rheology characterization of geopolymer nanocomposites used in 3D printing, Compos. B Eng. 176 (2019) 107290.
- [18] H. Xu, J.S.J. Van Deventer, The geopolymerisation of alumino-silicate minerals, Int. J. Miner. Process. 59 (2000) 247–266.
- [19] T.D. Ngo, A. Kashani, G. Imbalzano, K.T.Q. Nguyen, D. Hui, Additive manufacturing (3D printing): a review of materials, methods, applications and challenges, Compos Part B 143 (2018) 172–196.
- [20] P. Scanferla, A. Conte, A. Sin, G. Franchin, P. Colombo, The effect of fillers on the fresh and hardened properties of 3D printed geopolymer lattices, Open Ceram 6 (2021) 100134.
- [21] J. Archez, N. Texier-Mandoki, X. Bourbon, J.F. Caron, S. Rossignol, Shaping of geopolymer composites by 3D printing, J. Build. Eng. 34 (2021) 101894.
- [22] J. Zhong, G.X. Zhou, P.G. He, Z.H. Yang, D.C. Jia, 3D printing strong and conductive geo-polymer nanocomposite structures modified by graphene oxide, Carbon 117 (2017) 421–426.

- [23] M.T. Souza, L. Simão, E.G. de Moraes, L. Senff, J.R. de Castro Pessoa, M.J. Ribeiro, A.P. Novaes de Oliveira, Role of temperature in 3D printed geopolymers: evaluating rheology and buildability, *Mater. Lett.* 293 (2021) 129680.
- [24] J. Archez, N. Texier-Mandoki, X. Bourbon, J.F. Caron, S. Rossignol, Adaptation of the geopolymer composite formulation to the shaping process, *Mater. Today Commun.* 25 (2022), 101501.
- [25] W. N'cho, A. Gharzouni, J. Jouin, A. Aimable, I. Sobrados, S. Rossignol, Effet of mixing metakaolins: methodological approach to estimate metakaolin reactivity, *Ceram. Int.* 49 (2023) 20334–20342.
- [26] W.C. N'cho, A. Gharzouni, J. Jouin, S. Rossignol, Impact of different metakaolin mixtures on oligomer formation and geopolymer properties: impurity effect, *Open Ceram* 15 (2023) 100411.
- [27] A. Autef, E. Joussein, G. Gasgnier, S. Rossignol, Role of the silica source on the geopolymerization rate: a thermal analysis study, *J. Non-Cryst. Solids* 366 (2013) 13–21.
- [28] E. Prud'homme, P. Michaud, E. Joussein, J.M. Clacens, S. Rossignol, Role of alkaline cations and water content on geomaterial foams: monitoring during formation, *J. Non-Cryst. Solids* 357 (2011) 1270–1278.
- [29] A. Gharzouni, E. Joussein, B. Samet, S. Baklouti, S. Rossignol, Effect of the reactivity of alkaline solution and metakaolin on geopolymer formation, *J. Non-Cryst. Solids* 410 (2015) 127–134.
- [30] D. Jonathan, H.A. Kavner, A.E. Shauble, D. Snyder, E.C. Manning, Polymerization of aqueous silica in H₂O–K₂O solutions at 25–200 °C and 1 bar to 20 kbar, *Chem. Geol.* 283 (2011) 161–170.
- [31] I. Halasz, M. Agarwal, R. Li, N. Miller, What can vibrational spectroscopy tell about the structure of dissolved sodium silicates? *Microporous Mesoporous Mater.* 135 (2010) 74–81.
- [32] M. Arnoult, C. Dupuy, M. Colas, J. Cornette, L. Duponchel, S. Rossignol, Determination of the reactivity degree of various alkaline solutions: a Chemometric Investigation, *Appl. Spectrosc. Rev.* 73 (2019) 1361–1369.
- [33] N. Zotov, I. Ebbsjö, D. Timpel, H. Keppler, Calculation of Raman spectra and vibrational properties of silicate glasses: comparison between Na₂Si₄O₄ and SiO₂ glasses, *Phys. Rev. B* 60 (1999).
- [34] P. Scanferla, A. Gharzouni, N. Texier-Mandoki, X. Bourbon, S. Rossignol, Effects of potassium-silicate, sands and carbonates concentrations on metakaolin-based geopolymers for high-temperature Applications, *Open Ceram* 10 (2022) 100257.
- [35] P. Duxson, J.L. Provis, G.C. Lukey, S.W. Mallicoat, W.M. Kriven, J.S.J. Van Deventer, Understanding the relationship between geopolymer composition, microstructure and mechanical properties, *Colloids Surf., A* 269 (2005) 47–58.
- [36] N. Essaidi, L. Laou, S. Yotte, L. Ulmet, S. Rossignol, Comparative study of the various methods of preparation of silicate solution and its effect on the geopolymerization reaction, *Results Phys.* 6 (2016) 280–287.
- [37] A. Gharzouni, I. Sobrados, E. Joussein, S. Baklouti, S. Rossignol, Predictive tools to control the structure and the properties of metakaolin based geopolymer materials, *Colloids Surf. A Physicochem. Eng. Asp.* 511 (2016) 212–221.
- [38] C. Dupuy, A. Gharzouni, N. Texier-Mandoki, X. Bourbon, S. Rossignol, Thermal resistance of argillite-based alkali-activated materials. Part 1: effect of calcination processes and alkali cation, *Mater. Chem. Phys.* 217 (2018) 323–333.